# 5

# Discrete Numerical Simulations of the Strength and Microstructure Evolution During Compaction of Layered Granular Solids

## 5.1. Introduction

Compaction of granular materials and powders is a very common practice in several engineering and manufacturing applications [HEC 61]. Powders can be compacted using roller compaction, where powders are forced through a pair of rotating rollers. Powders can also be compacted using direct compaction, where powders inside a die are compacted in the axial direction. One of the main purposes of powder compaction is to form solids such as pharmaceutical tablets and direct compaction is mostly the preferred method to form the tablets. A lot has been learned from prior experimental studies on tablet compaction, including relationship between porosity and compaction pressure [HEC 61], the effects of particle size on powder compaction [ADO 97, ALM 08, EIC 09, FIC 05, HER 07, KHO 13, MCK 82, PAT 07, SUN 06, SUN 08, YOH 15], the role of lubricants on compaction and tensile strength of tablets [ALM 08, SUN 06], to mention only a few.

Chapter written by Bereket YOHANNES, Marcial GONZALEZ and Alberto M. CUITIÑO.

*From Microstructure Investigations to Multiscale Modeling: Bridging the Gap,* First Edition.
Edited by Delphine Brancherie, Pierre Feissel, Salima Bouvier and Adnan Ibrahimbegović.

The above-mentioned studies focus only on monolayer tablets, in which the entire power bed is exposed to the same applied compaction pressure. In recent years, there was some progress in the areas of layered powder compacts, especially for bilayer pharmaceutical tablets [ABE 14]. Bilayer tablets are useful for controlled drug delivery of two different active ingredients [ABE 14, ABD 04], and separation of chemically incompatible drugs [DIV 11]. In layered powder compaction, layers are compacted in a sequential manner. For example, compaction of a bilayer tablet consists of the following steps:

1) Filling die with the first-layer particles;

2) Compacting the first-layer particles (i.e. application of the first-layer compaction force);

3) Removing the first-layer compaction force;

4) Filling die with the second-layer particles on top of the first-layer particles;

5) Compacting the two layers together to form the bilayer tablet (i.e. application of the second-layer compaction force);

6) Removing the second-layer compaction force;

7) Ejecting the tablet from the die.

If more layers are needed, the process is repeated without ejecting the compacted layers from the die.

The production of these layered (both bilayer and multilayered) tablets poses a challenge as the layered tablets are prone to fracture by delamination, usually along the interfaces between two layers, because of their inherent insufficient strength [AKS 13, KOT 12]. Thus, one of the main manufacturing challenges is to obtain tablets that do not fracture at the interface because of insufficient mechanical strength.

The mechanical strength of a bilayer tablet depends on many factors. Several researchers have experimentally investigated the factors that influence the mechanical strength of these tablets, particularly the mechanical strength at the interface of the layers.

Using axial tensile strength tester, Akseli *et al*. [AKS 13] experimentally studied the strength of bilayer tablets made up of microcrystalline cellulose (MCC) and starch powders (Figure 5.1(a)). They studied the effect of the first- and second-layer compaction forces on the mechanical strength of the tablets and types of failures associated with it. They showed that the tensile strength of the bilayer tablets increased as the second-layer compaction force is increased. The increase in the tensile strength with the compaction force is also true for monolayer tablets [ADO 97, YOH 15, YOH 16]. The most interesting finding from experiments conducted by Akseli *et al*. [AKS 13] is that the tensile strength of the tablets does not increase monotonically with the magnitude of the first-layer compaction force, when the second-layer force is kept constant. For lower first-layer compaction forces, the tensile strength increases as the first-layer compaction force is increased. However, at higher first-layer compaction forces, the tensile strength decreases as the first-layer compaction force is increased. The highest tensile strength was achieved when the first-layer compaction force was 4 kN for a 10 mm-diameter tablet of both MCC–MCC and MCC–starch bilayers. (MCC–MCC refers to a tablet where both the first and second layers are composed of MCC powder, while MCC–starch refers to a tablet where the first layer is MCC powder and the second layer is starch powder).

Kottala *et al*. [KOT 12] showed that the layer interface surface roughness also significantly influences the mechanical properties of the bilayer tablet. They found that high interfacial roughness and the interfacial curvature increase bonding between adjacent layers, which tend to increase the interfacial strength of the tablets. Both the interfacial surface roughness and interfacial curvature reduce when the first-layer compaction force is increased. Their study also showed that the layer sequence has a significant effect on the tensile strength of the tablets, such that the tablets with brittle material as the first layer attain higher interfacial strength. However, the presence of different materials between the adjacent layers can also cause fracture and split at the interface due to inhomogeneous residual stress distribution in

the layers [INM 07, INM 09]. Using a three-point bending experiment (Figure 5.1(b)), Podczeck and Al-Muti [POD 10, POD 06] showed that the modulus of elasticity and the size of particles influenced the overall strength of layered tablets/beams. They found that if the material forming the lower layer was more elastic, then the beam strength was reduced due to tension introduced into the system, acting especially at the layer interface and potentially causing partial or complete delamination. Larger differences in the particle size of the materials forming the tablet layers also resulted in an overall reduced tensile strength. In another flexure test experiment, Busignies *et al*. [BUS 13] showed that the fracture occurred at the interface or in the layers depending on the properties of the materials. In most cases, the highest tensile strength was obtained when the materials had similar elastic recovery. On the contrary, for materials with different elastic recoveries, the tensile strengths were reduced.

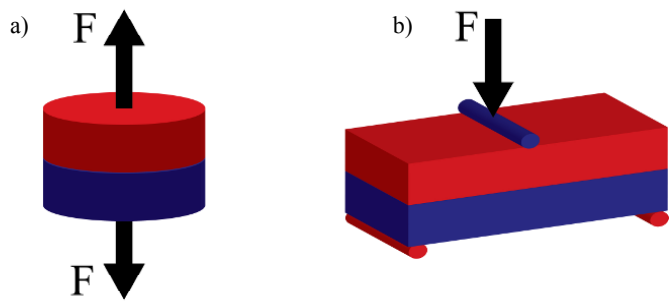


**Figure 5.1.** *Schematics of tensile strength tests for bilayer compacts: a) axial tensile strength test and b) three-point bending test*

Physical experiments can provide a lot of information about compaction of powders and the tensile strength of the compacts. However, in order to understand the evolution of the micromechanics, which occurs in the bulk of the powder bed, computational

simulations are required. The experimental results discussed in the previous section can also be used to validate the results of the computational models.

## 5.2. Numerical simulation

Several computational methods have been developed to model compaction of monolayer tablets. Some of these methods are based on finite element method (FEM) [KLI 10], discrete element method (DEM) [SHE 04, MAR 04, OLS 13, CUN 79], or combined discrete-finite element method (DFEM) [ZHE 02, ZHA 11, KOY 11]. In FEM, usually only the global values of the physical properties are assumed, while in DEM the interaction between individual particles are accounted for, which enables modeling the heterogeneity of powders at the microscopic/particle scale. Hence, DEM gives more accurate particle scale details than continuum methods that consider global physical properties of the material. The discrete particle methods have been used to model compaction and tensile strength of monolayer tablets. In this section, first, we will show important details of the discrete particle model elaborated in Yohannes *et al*. [YOH 16], and then we will present how the monolayer powder compaction models can be improved to model bilayer powder compaction.

### 5.2.1. *Discrete particle simulations of powder compaction*

DEM was originally developed for applications pertaining to very small elastic deformations for rock mechanics application [CUN 79]. Since then, the DEM has seen several improvement and applications in a variety of engineering and scientific areas including modeling of plastically deformed particles [SHE 04, MAR 04, OLS 13] and bonding between particles [POT 04], which are relevant for powder compactions. As the main difference between monolayer and bilayer tablets is the presence of layer interface in the latter case, these computational methods can be used to model bilayer tablets if the contact between particles at the layer interface are accounted for.

During the compaction, unloading and ejection simulation, the contact force between the particles is computed based on the deformation and mechanical properties of the particles. In the simulations, the deformation of particle is computed from the overlap between contacting particles, and the mechanical properties include the plastic, elastic and bonding properties of the particles. A pair of contacting particles can be in a loading mode (when the particles are in contact for the first time), or unloading mode (when the contact force on a pair of contacting particles is decreasing) or reloading mode (when previously contacting particles are overlapping again) [YOH 16]. During loading mode, the particles follow a power-law plasticity model [MAR 04, MES 00, STO 97, STO 99],

$$\sigma = k\epsilon^{1/m}, \qquad [5.1]$$

where $k$ and $m$ are particle plastic parameters, and $\epsilon$ and $\sigma$ are the strain and stress of the particles, respectively. The contact force (P) between two particles is then computed as

$$P = k_p a^{2+1/m}, \qquad [5.2]$$

where $a$ is the radius of the contact area between the pair of contacting particles, $a = \sqrt{2c_2 \frac{\gamma}{\frac{1}{R_1}+\frac{1}{R_2}}}$. $\gamma$ is the overlap between two contacting particles and $R$ is the radius of the particles. The subscripts 1 and 2 refer to the pair of contacting particles. $m$ is the average plastic parameter, $m = (m_1 + m_2)/2$. The parameter $k_p$ in [5.2] is given as

$$k_p = K\pi \left(\frac{1}{k_1^m}+\frac{1}{k_2^m}\right)^{-\frac{1}{m}} \left(\frac{1}{R_1}+\frac{1}{R_2}\right)^{\frac{-1}{2m}-1} (2C_2)^{1+\frac{1}{2m}}, \qquad [5.3]$$

where $K = 3 \times 6^{-1/m}$ and $c_2 = 1.43\exp\left(-\frac{0.97}{m}\right)$.

During the unloading of the contact force, P is computed as,

$$P = \frac{2k_p}{\pi} a_p^{2+1/m} \left[ \arcsin\left(\frac{a}{a_p}\right) - \frac{a}{a_p}\sqrt{1-\left(\frac{a}{a_p}\right)^2} \right] - \sqrt{8\pi\omega E_m}\, a_p^{\frac{3}{2}} \left(\frac{a}{a_p}\right)^{\frac{3}{2}}, \quad [5.4]$$

where $a_p$ is the radius of the contact area at the maximum $P$ during the loading phase, $\omega$ is the bonding energy per area and $E_m$ is the effective Young's modulus.

During compaction of a powder bed, which consists of many particles, the type of each contact is evaluated and the appropriate equation is used in order to compute the forces on the particles. The computational process involves finding the optimum configuration (position of each particle), such that the potential energy of the system is kept the minimum. Yohannes *et al*. [YOH 16] have shown that this method can be used to model compaction of powders and diametral tensile strength tests for monolayer tablets. Their simulation results were validated using physical experiments.

### 5.2.2. *Discrete particle simulation of layered compacts*

As mentioned earlier, the main difference between monolayer compacts and layered compacts is the interface between layers for the layered compacts. To model the interaction at the interface, Yohannes *et al*. [YOH 17] suggested a slight modification for the interaction of particles at the interface. The modification is based on the fact that the particles at the surface of the first layer have already been deformed due to the first-layer compaction force. When the first-layer force is removed, the elastic deformation is recovered, but the plastic deformation remains. To account for this deformation during the interaction of particles across the interface, Yohannes *et al*. [YOH 17] assumed the following: 1) the radius of first-layer particles at the surface is smaller than the original particle radius by the amount of the plastic deformation ($\gamma_p$) and 2) the elastically recovered region, which

is assumed as the "used part", cannot support any bonding. Then, the overlap of particles across the interface ($\gamma_{int}$) is computed as

$$\gamma_{int} = (R_f + R_s - \gamma_p) - (X_f - X_s) \cdot \mathbf{n_{fs}}, \quad [5.5]$$

where $R_f$ is the original particle size of the particle in the first layer, $R_s$ is the original particle size of the particle in the second layer, $\gamma_p$ is the plastic deformation of the first-layer particle due to the first-layer force, $X_f$ is the position vector of the center of the first-layer particle, $X_s$ is the position vector of the second-layer particle, and $n_{fs}$ is the unit normal vector between the centers of two particles.

Therefore, the contact force at the interface is developed only when $\gamma_{int} > 0$. For $0 < \gamma_{int} < \gamma_p$, it is assumed that the bonding between the particles is negligible and the contact force can only be compressive. If the contact is in a loading mode, [5.2] is used to compute the contact force, whereas, if the contact is in an unloading mode, the first term of [5.4] is used to compute the contact force. The bonding between the particles develops only when $\gamma_{int} \geq \gamma_p$. These assumptions about the interaction of particles, specifically the computation of the overlap for particles at the interface and the assumption about the bonding force between the particles, are the key factors that distinguish bilayer or multilayered tablets from monolayer tablets.

Simulations were run for lactose–lactose bilayer tablets based on these assumptions. Figure 5.2 shows the bilayer compaction process and the evolution of the bonding forces between contacting particles. Figure 5.2(a) shows the first layer being compacted and the bonding forces between particles of the first layer. The bonding between the particles still exists even after the first-layer compaction force is removed (Figure 5.2(b)). The bonding between the second-layer particles starts only after the second-layer force is applied (Figure 5.2(c)). Initially, the bonding force between the second-layer particles is much smaller than that between the first-layer particles. At the end of the compaction process, the bonding between particles of the first and second layers becomes almost equivalent (Figure 5.2(d)). These and other quantitative details are discussed in the next section.

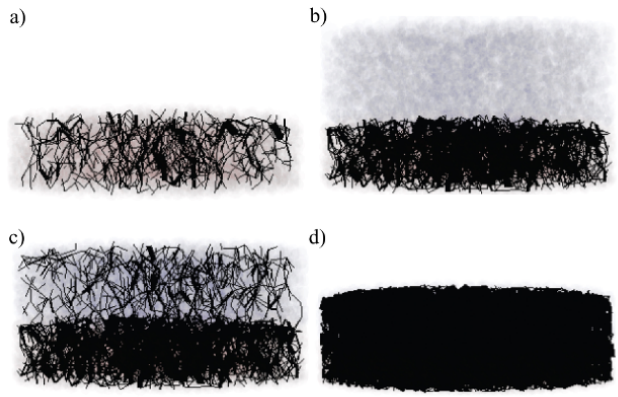


**Figure 5.2.** *The bonding force between particles: a) during compaction of the first layer; b) after the first layer is removed and second-layer particles are deposited on top of the first-layer particles; c) during the application of the second-layer force and d) at the maximum second-layer force. The thickness of the lines represents the magnitude of the bonding force between the particles*

## 5.3. Discussion

As mentioned in the previous section, one of the main advantages of the discrete particle method is that we can track the contact forces on each particle in detail. In this section, we present comparisons between contact forces and contact areas inside the two layers and at the interface of the layers. One way of checking the heterogeneity in the micromechanics of the tablet is to compute the probability distribution function (pdf) of the contact forces. Figure 5.3(b) shows the distribution of the contact forces inside the layers and at the interface of the layers for a lactose–lactose bilayer tablet after the tablet is ejected from the die. The contact forces at the layer interface are computed from all contacts between the first-layer and the second-layer particles. To have a reasonable comparison between the forces in the layers and at the interface, we only consider the contact forces across a given plane in the layers (Figure 5.3(a)). Though there is no external force applied on the tablet after ejection, there still exist some residual contact forces between the particles. From equilibrium criteria, we understand the summation of all these residual forces to be zero. In addition, we note that the distributions of the contact forces are similar for both layers and at the interface. The maximum

compressive contact force is approximately 2 N and the maximum tensile force is about –1.2 N. The distribution resembles a Gaussian distribution with a mean around zero. The similarity in the contact forces indicates that there is no statistically noticeable difference between the contact forces.

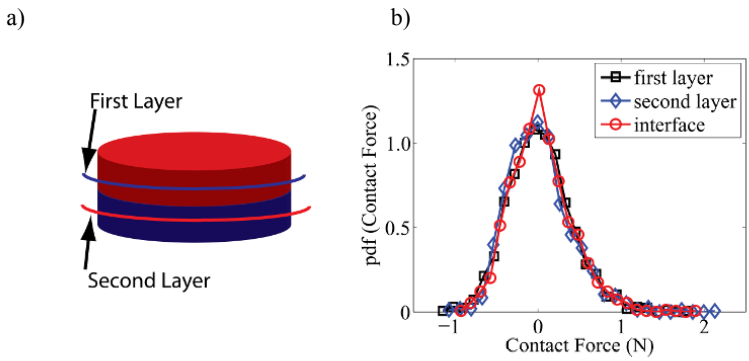


**Figure 5.3.** *a) Schematics that shows the planes at which the contact forces are computed and b) the distribution of contact forces in the first layer, second layer and at the interface for lactose–lactose bilayer after the tablet is ejected. Compressive forces are +ve and tensile forces are –ve. For a color version of the figure, see www.iste.co.uk/brancherie/microstructure.zip*

In addition to the pdf of the contact forces, we can also look into the orientation of the contact forces to investigate any preferential orientation of the contacts in the layers and at the interface. Figure 5.4 shows polar plots that represent the orientation and the magnitude of the contact forces. As shown in the schematics in Figure 5.4, the z-axis is along the axial direction, which is the direction of the applied compaction force. The horizontal plane is formed by the x–y axes. The orientation and the magnitude of the contact forces in the layers (only the result in the second layer is shown here) and at the layer interface are similar. The compressive forces (Figure 5.4(a) and (c)) have a maximum value of approximately 12 N mostly aligned between $30^{o}$ and $60^{o}$, and symmetrical about z-axis and xy-plane. On the other hand, most of the tensile contact forces (Figure 5.4(b) and (d)) are aligned between $0^{o}$ and $60^{o}$, which is also symmetrical about the z-axis and xy-plane for both layers and at the interface. These results are very similar to the orientation contact forces reported by Yohannes *et al*. [YOH 16] for monolayer compacts.

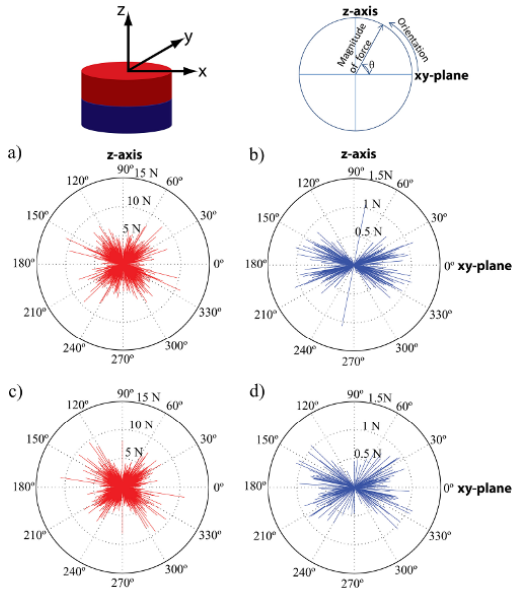


**Figure 5.4.** *The orientation of compressive and tensile contact forces in the second layer and at the interface during the maximum compaction force (relative density = 1.0): a) compressive contact force in the second layer, b) tensile contact force in the second layer, c) compressive contact force at the interface and d) tensile contact force at the interface. For a color version of the figure, see www.iste.co.uk/brancherie/microstructure.zip*

These contact forces do not represent the bonding between the particles. The bonding between the particles is equivalent to the force that is required to break the contact between the particles. The bonding force can be computed numerically from [5.4] or by taking the derivative of the equation with respect to the plastic contact radius $a_p$. Figure 5.5 shows the pdf of the bonding force between particles in the layers and at the interface. The bonding forces are computed in the regions as shown earlier in Figure 5.3(a). The bonding force ranges between 0 and –2.5 N. The distribution of the bonding force in the layers and at the interface is similar.

Based on the result presented in Figures 5.3–5.5, we can see that the distribution, orientation and the magnitude of the contact forces and bonding force are not sufficient to describe the difference in the tensile strength between the layers and at the interface. These

quantities behave similarly at any point in the bilayer tablet. Perhaps, the appropriate measure of tensile strength is a cumulative measure of the bonding *forces*, which can be represented by the total bonding *area*. From our discrete particle simulations, the bonding area can be computed for all contacts between particles. Here, as described in section 5.2.2, we want to distinguish between the total contact area and the bonding area. The contact area is the total contact area between the particles; however, the existence of a contact area does not guarantee bonding between particles particularly for deformed particles of the first-layer particles at the layer interface.

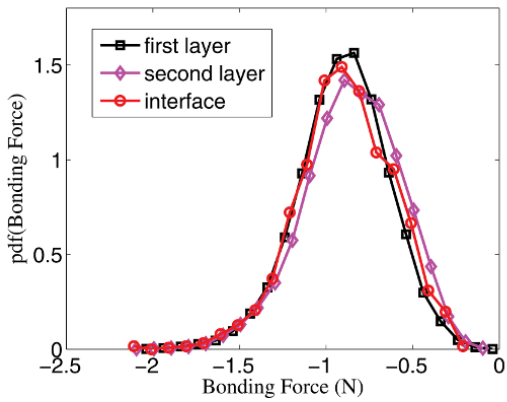


**Figure 5.5.** *The distribution of the bonding force in the first layer, second layer and at the layer interface for a bilayer tablet. For a color version of the figure, see www.iste.co.uk/brancherie/microstructure.zip*

In Figure 5.6, we show the contact area and bonding area for first-layer compaction pressures of 30 MPa, 60 MPa and 90 MPa. The contact area is normalized by the cross-sectional area of the smallest particle used in the simulation, which has a radius of 50 μm. In general, both the contact area and bonding area increase as the relative density of the tablets increases (relative density is computed as 1.0 – porosity). The increase in relative density corresponds to the increase in the second-layer pressure. For these tablets, a relative density of 1.0 corresponds to a second-layer pressure of approximately 250 MPa. The first layer has a higher contact and bonding area during the early stages of the application of the second-layer force. The area is higher

because, as explained in section 5.2.2, the first layer has been already compacted during the application of the first-layer pressure. The contact area in the first layer increases by a factor of two when the first-layer compaction pressure is increased from 30 MPa to 90 MPa (compare Figure 5.6(a) and (e)). The initial contact area in the second layer and at the interface is zero since the second-layer pressure is not applied yet. The contact area in the second layer and at the interface increases continuously as the second-layer compaction pressure is applied, whereas the contact area in the first layer remains almost constant at the early stages of the application of the second-layer pressure. Once the contact areas in the second layer and at the interface approach the contact area in the first layer, the contact areas in the layers and at the interface increase at the same rate.

The bonding area is almost the same as the contact area for the first- and second-layer particles. However, the bonding area at the interface is less than the contact area, particularly when the first-layer pressure is 90 MPa. The lower bonding area indicates that the tensile strength at the interface is weaker at the interface. This result is similar to the experimental findings of Akseli *et al*. [AKS 13], in which they reported that, for higher first-layer compaction pressures, the bilayer tablets break at the interface during the axial tensile strength test. Actually, the tablets break at the interface with a pure delamination-type failure. For lower first-layer compaction pressures, Akseli *et al*. [AKS 13] found that the tablets could break in the first layer or second layer or at the interface, which, again, corresponds to our results where the bonding areas in the layers and at the interface are almost the same (e.g. Figure 5.6(b), when the first-layer pressure is 30 MPa). Had we considered only the contact areas, the simulations would not be able to predict the difference in the tensile strength of the layers and the interface.

Along the reduced area due to plastic deformation of the first-layer particles, the roughness of the first-layer surface plays an important role in the tensile strength of layered compacts [KOT 12]. Higher roughness provides more contact and bonding area at the interface. The roughness at the interface decreases as the magnitude of the first-layer compaction force is increased, since higher compaction forces

cause significant particle rearrangement and deformation. Therefore, at higher first-layer compaction pressure, the contact area is further reduced by the smoothness of the top surface of the first layer. Actually, using the numerical model described here, Yohannes *et al*. [YOH 17] showed that the maximum bonding area is achieved at intermediate first-layer compaction pressure.

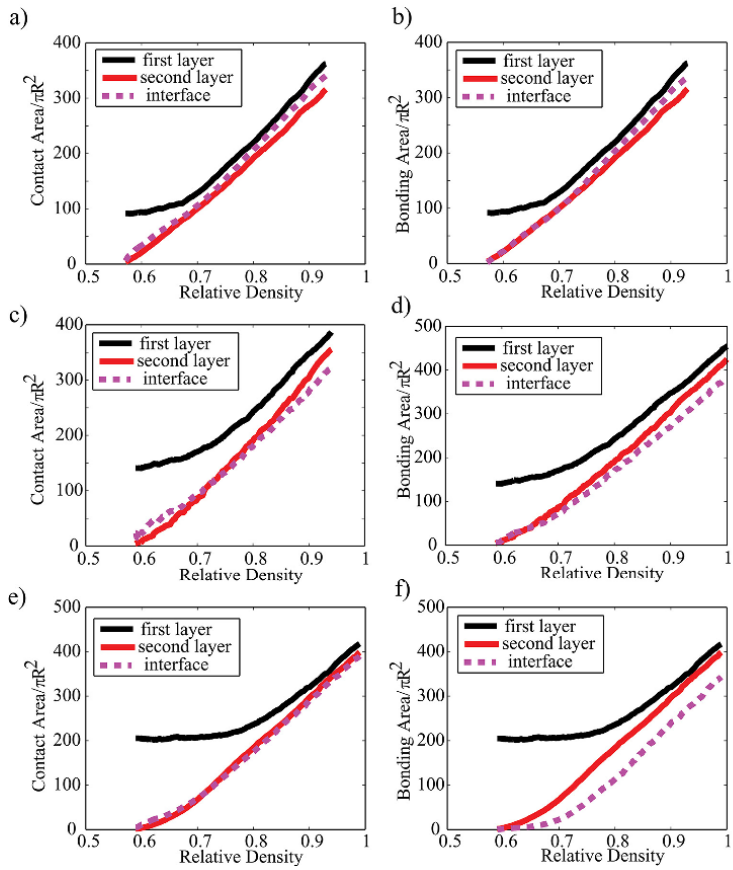


**Figure 5.6.** *Evolution of contact area and bonding area during the application of second-layer force. The tablets were compacted up to a relative density of 1.0, which corresponds to a second-layer pressure of 250 MPa. The first-layer pressure was 30 MPa for a) and b), 60 MPa for c) and d), and 90 MPa for e) and f). R is the radius of the smallest particle used in the simulations, which is 50 μm. For a color version of the figure, see www.iste.co.uk/brancherie/microstructure.zip*

## 5.4. Conclusion

We presented a discrete particle-based modeling of bilayer powder compacts. The model is an extension of a model implemented earlier by Yohannes *et al*. [YOH 16] for monolayer tablets. The model for the bilayer powder compaction takes into consideration the plastic deformation of the first-layer particles, which were in direct contact with the punch during the application of the first-layer compaction pressure.

Using this model, we were able to show that the bonding area at the interface is significantly reduced for high first-layer compaction pressures. This reduced bonding area is the main cause of weak tensile strength at the interface, which was also observed in experiments. The reduced roughness at higher first-layer compaction pressures at the interface also plays an important role in reducing the tensile strength further. Despite the differences in the bonding area, other statistical parameters such as the distribution of the contact forces, the distribution of the bonding forces, and the orientation of the contact forces in the layers and at the interface are similar. Further, this model can be easily extended to multilayered powder compacts by repeating the model for deformation of the first-layer particles discussed in section 5.2.2 for all the layers.

## 5.5. Acknowledgements

We thank Admassu Abebe, Faranak Nikfar and Omar Sprockel for their fruitful discussions.

## 5.6. Bibliography

[ABD 04] ABDUL S., PODDAR S., "A flexible technology for modified release of drugs: multi layered tablets", *Journal of Controlled Release*, vol. 97, no. 3, pp. 93–405, 2004.

[ABE 14] ABEBE A., AKSELI I., SPROCKEL O. *et al.*, "Review of bilayer tablet technology", *International Journal of Pharmaceutics*, vol. 461, no. 12, pp. 549–558, 2014.

[ADO 97] ADOLFSSON A., Olsson H., Nystrom C., "Effect of particle size and compaction load on inter-particulate bonding structure for some pharmaceutical materials studied by compaction and strength characterization in butanol", *European Journal of Pharmaceutics and Biopharm*, vol. 44, pp. 243–251, 1997.

[AKS 13] AKSELI I., ABEBE A., SPROCKEL O. *et al.*, "Mechanistic characterization of bilayer tablet formulations", *Powder Technology*, vol. 236, pp. 30–36, 2013.

[ALM 08] ALMAYA A., ABURUB A., "Effect of particle size on compaction of materials with different deformation mechanisms with and without lubricants", *AAPS PharmSciTech*, vol. 9, no. 2, pp. 414–418, 2008.

[BUS 13] BUSIGNIES V., MAZEL V., DIARRA H. *et al.*, "Role of the elasticity of pharmaceutical materials on the interfacial mechanical strength of bilayer tablets", *International Journal of Pharmaceutics*, vol. 457, no. 1, pp. 260–267, 2013.

[CUN 79] CUNDALL P.A., STRACK O.D.L., "A discrete numerical model for granular assemblies", *Géotechnique*, vol. 29, pp. 47–65, 1979.

[DIV 11] DIVYA A., KAVITHA K., KUMAR M.R. *et al.*, "Bilayer tablet technology: an overview", *Journal of Applied Pharmaceutical Science*, vol. 1, pp. 43–47, 2011.

[EIC 09] EICHIE F.E., KUDEHINBU A.O., "Effect of particle size of granules on some mechanical properties of paracetamol tablets", *African Journal of Biotechnology*, vol. 8, no. 21, pp. 5913–5916, 2009.

[FIC 05] FICHTNER F., KE RASMUSON A., ALDERBORN G., "Particle size distribution and evolution in tablet structure during and after compaction", *International Journal of Pharmaceutics*, vol. 292, pp. 211–225, 2005.

[HEC 61] HECKLE R.W., "Density-pressure relationships in powder compaction", *Transactions of the Metallurgical Society of AIME*, vol. 221, pp. 671–675, 1961.

[HER 07] HERTING M.G., KLEINEBUDDE P., "Roll compaction/dry granulation: effect of raw material particle size on granule and tablet properties", *International Journal of Pharmaceutics*, vol. 338, pp. 110–118, 2007.

[INM 07] INMAN S., BRISCOE B., PITT K., "Topographic characterization of cellulose bilayered tablets interfaces", *Chemical Engineering Research and Design*, vol. 85, no. 7, pp. 1005–1012, 2007.

[INM 09] INMAN S., BRISCOE B., PITT K. *et al.*, "The non-uniformity of microcrystalline cellulose bilayer tablets", *Powder Technology*, vol. 188, no. 3, pp. 283–294, 2009.

[KHO 13] KHOMANE K.S., BANSAL A.K., "Effect of particle size on in-die and out-of-die compaction behavior of ranitidine hydrochloride polymorphs", *AAPS PharmSciTech*, vol. 14, no. 3, pp. 1169–1177, 2013.

[KLI 10] KLINZING G.R., ZavaLiangos A., CUNNINGHAM J. *et al.*, "Temperature and density evolution during compaction of a capsule shaped tablet", *Computers and Chemical Engineering*, vol. 34, no. 7, pp. 1082–1091, 2010.

[KOT 12] KOTTALA N., ABEBE A., SPROCKEL O. *et al.*, "Influence of compaction properties and interfacial topography on the performance of bilayer tablets", *International Journal of Pharmaceutics*, vol. 436, no. 12, pp. 171–178, 2012.

[KOY 11] KOYNOV A., AKSELI I., CUITIÑO A.M., "Modeling and simulation of compact strength due to particle bonding using hybrid discrete-continuum approach", *International Journal of Pharmaceutics*, vol. 418, pp. 273–285, 2011.

[MAR 04] MARTIN C., BOUVARD D., "Isostatic compaction of bimodal powder mixtures and composites", *International Journal of Mechanical Sciences*, vol. 46, no. 6, pp. 907–927, 2004.

[MCK 82] MCKENNA A., MCCAFFERTY D.F., "Effect of particle size on the compaction mechanism and tensile strength of tablets", *Journal of Pharmacy and Pharmacology*, vol. 34, no. 6, pp. 347–351, 1982.

[MES 00] MESAROVIC S.D., JOHNSON K., "Adhesive contact of elastic-plastic spheres", *Journal of the Mechanics and Physics of Solids*, vol.48, no. 10, pp. 2009–2033, 2000.

[OLS 13] OLSSON E., LARSSON P.-L., "A numerical analysis of cold powder compaction based on micromechanical experiments", *Powder Technology*, vol. 243, pp. 71–78, 2013.

[PAT 07] PATEL S., KAUSHAL A., BANSAL A., "Effect of particle size and compression force on compaction behavior and derived mathematical parameters of compressibility", *Pharmaceutical Research*, vol. 24, no. 1, pp. 111–124, 2007.

[POD 06] PODCZECK F., DRAKE K., NEWTON J. *et al.*, "The strength of bilayered tablets", *European Journal of Pharmaceutical Sciences*, vol. 29, pp. 361–366, 2006.

[POD 10] PODCZECK F., AL-MUTI E., "The tensile strength of bilayered tablets made from different grades of microcrystalline cellulose", *European Journal of Pharmaceutical Sciences*, vol. 41, no. 34, pp. 483–488, 2010.

[POT 04] POTYONDY D.O., CUNDALL P.A., "A bonded-particle model for rock", *International Journal of Rock Mechanics and Mining Sciences*, vol. 41, no. 8, pp. 1329–1364, 2004.

[SHE 04] SHENG Y., LAWRENCE C., BRISCOE B. *et al.*, "Numerical studies of uniaxial powder compaction process by 3d dem", *Engineering Computations*, vol. 21, pp. 304–317, 2004.

[STO 97] STORÅKERS B., BIWA S., LARSSON P.-L., "Similarity analysis of inelastic contact", *International Journal of Solids and Structures*, vol. 34, no. 24, pp. 3061–3083, 1997.

[STO 99] STORÅKERS B., FLECK N., MCMEEKING R., "The viscoplastic compaction of composite powders", *Journal of the Mechanics and Physics of Solids*, vol. 47, no. 4, pp. 785–815, 1999.

[SUN 06] SUN C.C., HIMMELSPACH M.W., "Reduced tabletability of roller compacted granules as a result of granule size enlargement", *Journal of Pharmaceutical Sciences*, vol. 95, no. 1, pp. 200–206, 2006.

[SUN 08] SUN C.C., "On the mechanism of reduced tabletability of granules prepared by roller compaction", *International Journal of Pharmaceutics*, vol. 347, pp. 171–172, 2008.

[YOH 15] YOHANNES B., GONZALEZ M., ABEBE A. *et al.*, "The role of fine particles on compaction and tensile strength of pharmaceutical powders", *Powder Technology*, vol. 274, pp. 372–378, 2015.

[YOH 16] YOHANNES B., GONZALEZ M., ABEBE A. *et al.*, "Evolution of the microstructure during the process of consolidation and bonding in soft granular solids", *International Journal of Pharmaceutics*, vol. 503, pp. 68–77, 2016.

[YOH 17] YOHANNES B., GONZALEZ M., ABEBE A. *et al.*, "Discrete particle modeling and micromechanical characterization of bilayer tablet compaction", *International Journal of Pharmaceutics*, vol. 529, pp. 597–607, 2017.

[ZHA 11] ZHANG J., ZAVALIANGOS A., "Discrete finite-element simulation of thermoelectric phenomena in spark plasma sintering", *Journal of Electronic Materials*, vol.40, no. 5, pp. 873–878, 2011.

[ZHE 02] ZHENG S., CUITIÑO A.M., "Consolidation behavior of inhomogeneous granular beds of ductile particles using a mixed discrete-continuum approach", *KONA Powder and Particle Journal*, vol. 20, pp. 168–177, 2002.